

ARTICLES

Equation of state for hydrogen below 10000 K: From the fluid to the plasma

Dieter Beule, Werner Ebeling, and Andreas Förster

Institut für Physik, Humboldt-Universität zu Berlin, Invalidenstraße 110, D-10115 Berlin, Germany

Hauke Juranek, Stefan Nagel, Ronald Redmer, and Gerd Röpke

Fachbereich Physik, Universität Rostock, Universitätsplatz 3, D-18051 Rostock, Germany

(Received 11 December 1998)

We combine equations of state valid for the dense, neutral fluid and the dense, fully ionized plasma to obtain an equation of state for the intermediate region where partial dissociation and ionization occur. A region of thermodynamic instability is found which is known as plasma phase transition. The corresponding coexistence region and the coexistence line are derived. As a first application of the new equation of state, Hugoniot curves are calculated and compared with experiments and other theories. [S0163-1829(99)09821-5]

I. INTRODUCTION

Knowledge of the equation of state (EOS) of dense hydrogen is of central importance for astrophysics as well as for the general understanding of the behavior of matter at extreme conditions. At low temperatures and pressures, hydrogen is a molecular solid or fluid. At high pressures above 100 GPa, hydrogen is supposed to undergo a transition to a highly conducting state which has been verified experimentally in shock-compressed fluid around 140 GPa and 3000 K.¹ Similar conductivity data have been reported recently for the high-pressure fluid domain.²

The physical nature of this transition at extreme conditions remains still unexplained. The interesting question—whether or not this transition is accompanied by a first-order phase transition with a corresponding instability region, a coexistence line, and a critical point—has been treated within advanced many-particle methods adopting a chemical picture (see, e.g., Refs. 3–7). There, the different components in a dense, partially ionized plasma such as molecules H₂, atoms H, molecular ions H₂⁺ or H⁻, electrons *e*, and protons *p* interact via effective pair potentials. It was found that the theoretical results for the EOS in that region depend strongly on the effective interactions for the neutral components, molecules, and atoms as well as on the Coulomb interactions between the charged particles.

Applying concepts of solid state theory, the observed transition can be explained by band gap closure, not accompanied by a first-order phase transition (for a review, see Ref. 8). Band structure calculations which are strictly valid only for the solid at *T*=0 K were performed for various structures. Comparing the energies of a hypothetical bcc metal with a close-packed lattice of hydrogen atoms or molecules interacting via effective short-range potentials, the metallic structure becomes more stable than the molecular solid at high densities. Furthermore, the atomic solid has always a higher energy than the metallic solid.

Ross⁹ adjusts this picture for the solid at *T*=0 K to the case of a shock-compressed liquid at finite temperatures, supposing that partially dissociated hydrogen fluid is a mix-

ture of a molecular and a metallic phase. The free energy of the fluid mixture is determined by a composition average of the free energy of the pure molecular and metallic phases within the linear mixing approximation.

Alternatively, the behavior of dense hydrogen is derived from numerical simulations, which treat a system consisting of a finite number of electrons and protons, starting with early quantum Monte Carlo calculations.¹⁰ Modern methods like quantum molecular dynamics,^{11,12} wave-packet molecular dynamics,^{13,14} or path-integral Monte Carlo^{15,16} allow one to study equilibrium as well as transport properties of dense hydrogen. In some of these simulations, precursors of a first-order phase transition, have been obtained.^{10,14,16}

We present in this paper an EOS for dense, low-temperature hydrogen plasma by combining earlier results for the partially and fully ionized plasma domain^{3,17–19} with improved data for the dense, neutral fluid obtained within a dissociation model.^{20,21} Results for the dissociation and ionization degree, the equation of state, the instability region, and the coexistence line are given for temperatures *T* = (2–10) × 10³ K and densities up to 1.1 g/cm³.

II. EOS FOR DENSE HYDROGEN

The EOS employed in this paper is based on the free energy density $f = F/V$ for a two-component system of neutral (index 0) and charged particles (index \pm),

$$f = f_0 + f_{\pm}. \quad (1)$$

We take into account in an explicit way the interactions in the neutral and charged subsystems, respectively, whereas the interaction between charges and neutrals is accounted for only by the reduced-volume concept.^{18,22}

We have performed classical Monte Carlo simulations for neutral, partially dissociated, fluid hydrogen for a grid of temperature and density points in the parameter region *T* = (2–10) × 10³ K and 0.2 g/cm³ ≤ ρ_0 ≤ 1.1 g/cm³ where ρ_0 denotes the total mass density of the neutral particles. Effec-

TABLE I. Coefficients of the interpolation formulas (3) and (4). The pressure is obtained in GPa and the free energy density in GJ/m³ when inserting the temperature in units of 10⁴ K and the density in g/cm³.

i	c_{i0}	c_{i1}	C_{i0}	C_{i1}
2	2055	-335.1	688.2	-198.6
3	0	388.2	2395	0
4	-2469	0	0	0
5	547.2	0	0	0

tive pair potentials of the exponential-6 form have been used to model the interactions between the molecules and atoms in the dense fluid.²³ The dissociation equilibrium $\text{H}_2 \rightleftharpoons 2 \text{H}$ has been solved, taking into account the correlation parts of the chemical potentials using fluid variational theory (for details, see Refs. 20 and 21). Dissociation becomes already important in the dense fluid above 20 GPa due to the lowering of the dissociation energy with increasing density. The degree of dissociation β is defined via $\beta = n_{\text{H}}/n_0$, where $n_0 = n_{\text{H}} + 2n_{\text{H}_2}$ is the total number density of hydrogen nuclei in the neutral component; n_{H} and n_{H_2} are the partial densities of atoms and molecules, respectively.

We have shown previously²⁰ that the results for the pressure of the neutral fluid as a function of density are in reasonable agreement with the available shock-wave experiments¹ that have reached temperatures around 3000 K and with the similar linear-mixing model of Ross.⁹ For densities and temperatures leading to a low degree of dissociation the pressure agrees well with the data given by Saumon and Chabrier.⁴ These authors have used a stiffer atom-atom potential and, as discussed in Refs. 21 and 25, systematic deviations occur with an increasing fraction of dissociated molecules for higher temperatures and/or densities.

The resulting pressure of the neutral subsystem p_0 can be split into the ideal contributions of the atoms and molecules and an interaction contribution,

$$p_0 = \frac{\beta \rho_0 k_B T}{m_{\text{H}}} + \frac{(1-\beta) \rho_0 k_B T}{2m_{\text{H}}} + p_0^{\text{int}}(\rho_0, T). \quad (2)$$

The Monte Carlo data can be interpolated accurately using an expansion of the interaction contribution with respect to the density and temperature according to

$$p_0^{\text{int}}(\rho_0, T) = \sum_{i \geq 2, j} (c_{ij} T^{j/2} \rho_0^i + C_{ij} T^{j/2} \rho_0^i \ln \rho_0). \quad (3)$$

The advantage of the expansion (3) is that all other thermodynamic quantities are now at hand in a similar analytical form. An eight-parameter fit with $i=2,3,4,5$ and $j=0,1$ is sufficient to reproduce the Monte Carlo data within typical errors of less than 4% for the pressure and less than 0.4 eV/atom for the internal energy within the region $T = (2-10) \times 10^3$ K and $0.2 \text{ g/cm}^3 \leq \rho_0 \leq 1.1 \text{ g/cm}^3$. The respective coefficients, derived from a simultaneous least-squares fit of the pressures and internal energy densities at 57 grid points in the density-temperature region given above, are listed in Table I. For the free energy density of the neutral subsystem we obtain

$$f_0 = f_0^{\text{id}} + f_0^{\text{int}},$$

$$f_0^{\text{int}} = \sum_{i \geq 2, j} \left\{ c_{ij} \frac{T^{j/2} \rho_0^i}{i-1} + C_{ij} \frac{T^{j/2} \rho_0^i}{(i-1)^2} [(i-1) \ln \rho_0 - 1] \right\}. \quad (4)$$

The ideal part depends on the dissociation equilibrium,

$$f_0^{\text{id}} = n_{\text{H}} k_B T \left[\ln \left(\frac{n_{\text{H}} \Lambda_{\text{H}}^3}{\sigma_{\text{PBL}}} \right) - 1 \right] + n_{\text{H}_2} k_B T \left[\ln \left(\frac{n_{\text{H}_2} \Lambda_{\text{H}_2}^3}{\sigma_{\text{H}_2}} \right) - 1 \right]. \quad (5)$$

The thermal de Broglie wavelength for species ν with mass m_ν is defined by $\Lambda_\nu = h/\sqrt{2\pi m_\nu k_B T}$. The excited states of the atoms are accounted for by the Planck-Brillouin-Larkin partition function²⁶

$$\sigma_{\text{PBL}}(T) = \sum_{s \geq 1} 4s^2 \left[\exp \left(\frac{I}{k_B T s^2} \right) - 1 - \frac{I}{k_B T s^2} \right], \quad (6)$$

where $I = 13.598$ eV is the ionization energy of hydrogen atoms in the ground state. The molecular partition function consists of a binding, a rotational, and a vibrational part,

$$\sigma_{\text{H}_2} = \frac{16k_B T/hcB}{1 - \exp(-hc\omega/k_B T)} \exp \left(\frac{2I + D_0 + hc\omega/2}{k_B T} \right) + \text{contribution of excited electronic states}, \quad (7)$$

where $B = 60.853 \text{ cm}^{-1}$, $\omega = 4401 \text{ cm}^{-1}$, and $D_0 = 4.735$ eV; see Ref. 20.

The free energy density of the charged component is split in a similar way as Eq. (4):

$$f_{\pm} = f_{\pm}^{\text{id}} + f_{\pm}^{\text{int}} = f_e^{\text{id}*} + f_i^{\text{id}} + f_e^* + f_i + f_{ie}. \quad (8)$$

f_e^{id} and f_i^{id} denote the ideal contribution of the electrons and ions as derived from Fermi-Dirac and Boltzmann statistics, respectively. The interaction contributions f_e and f_i account for the correlations and the exchange in the electronic and ionic subsystem, while f_{ie} describes the electron-ion screening. They are treated in terms of Padé approximations^{3,17} which are based on analytical results for the quantum virial expansion²⁶ and are given and discussed in detail in Ref. 18. In comparison to these formulas, we have used an improved expression for the electronic contribution f_e by considering additional thermal corrections.²⁷ At low densities and/or high temperatures, the Padé approximations reproduce the quantum corrections to the Debye law. With increasing density, ions and electrons behave in quite different ways. The ions form a subsystem of classical, strongly coupled particles with a latticelike structure screened by a partially degenerate electron liquid. There, the present Padé approximation converges to the results of respective Monte Carlo simulations for the ion-ion and ion-electron interactions. The analysis performed in Ref. 27 yields also good agreement with the quantum Monte Carlo simulations available so far.¹⁵

The asterisk in Eq. (8) indicates that the corresponding expression is rescaled according to the concept of reduced volume for the free electrons.^{19,22} This means in brief that the accessible system volume is reduced by the hard-sphere volumes of atoms and molecules. The effective hard-sphere ra-

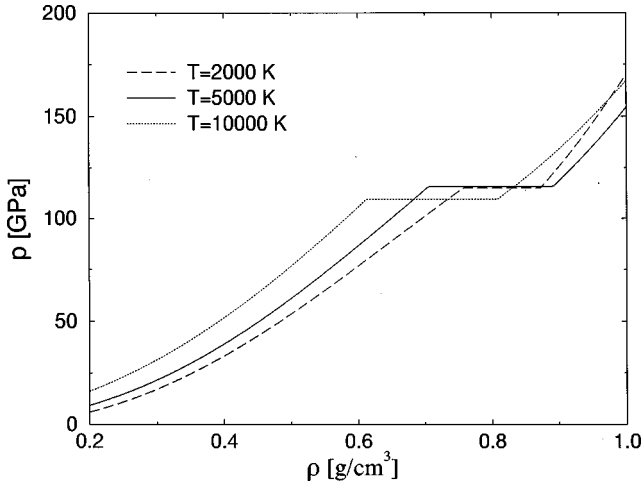


FIG. 1. Pressure as function of the density for various temperatures. A Maxwell construction was performed in the instability region, leading to constant pressure in the coexistence region.

dii are determined within fluid variational theory for the respective one-component systems. There, the free energy is obtained by minimizing a free energy functional with respect to the packing fraction of a hard-sphere reference system.²³ This way density- and temperature-dependent hard-sphere radii are derived.

III. RESULTS

Based on the formulas given above, the ionization equilibrium of the plasma was calculated by minimizing the total free energy. In the density region where the EOS shows an instability, i.e., $(\partial p/\partial V)_T > 0$, a Maxwell construction in terms of the pressure and the chemical potential was applied,

$$p(\rho_I, T) = p(\rho_{II}, T) \quad \text{and} \quad \mu(\rho_I, T) = \mu(\rho_{II}, T), \quad (9)$$

where $\mu = \mu_e + \mu_i = \mu_H = \mu_{H_2}/2$ is the combined chemical potential.¹⁹ Figure 1 shows the results for the EOS $p(\rho, T)$. As the pressure is primarily caused by correlation effects, the density dependence is much more pronounced than the temperature dependence. The phase transition which occurs in our model is well known as the *plasma phase transition* (PPT). In the coexistence region below 10000 K, the plasma consists of two phases I and II that differ in mass densities by about 0.2 g/cm^3 . The densities of the coexisting phases ρ_I and ρ_{II} have the general tendency to decline with the temperature. The PPT is characterized by a jump in the mass density, in the degree of ionization, and in the degree of dissociation. In the temperature region studied here, phase I is an atomic-molecular fluid with almost no ionization while phase II is a partially ionized plasma. The transition pressure is decreasing with the temperature and varies between 120 GPa and 110 GPa for $T = (2-10) \times 10^3 \text{ K}$. Figure 2 shows the respective coexistence line $p^{\text{PPT}}(T)$ of the two phases as well as lines of constant degree of dissociation and ionization. The degree of ionization α is defined as the mass fraction of the charged particles. In the partially dissociated fluid below the coexistence line it is always lower than 10^{-4} . Correspondingly, the conductivity is rather low, describing a semiconducting behavior. Crossing the coexistence line, the

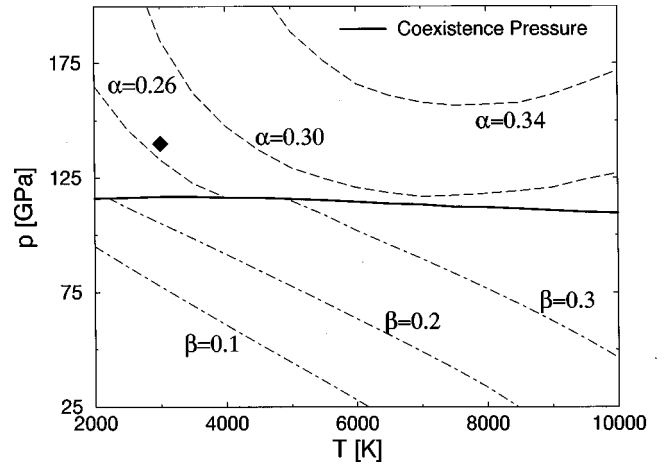


FIG. 2. Coexistence pressure and lines of constant degree of dissociation β and ionization α , respectively, as function of the temperature. The conditions where Weir *et al.* (Ref. 1) observed metallic conductivity are indicated by a diamond.

degree of ionization jumps to a value of about one-third which is connected with a rather high, plasmalike conductivity. Therefore, the behavior of the electrical conductivity as found in the multiple shock experiments¹ is qualitatively reproduced using the present EOS as shown in Ref. 28. Figure 3 shows the density region where the two phases coexist; the coexistence region is rather narrow. The experimental point where Weir *et al.*¹ observed a metal-like conductivity lies above the present coexistence line, supporting our result of considerable ionization in this region.

At much lower temperatures in the solid phase, a transition from the molecular crystal to hydrogen metal is commonly expected. Although solid metallic hydrogen has not yet been observed in diamond anvil cell experiments,²⁹ metallization is likely to occur above 300 GPa. For higher temperatures $T \geq 10^4 \text{ K}$ in the plasma state, the location of the PPT has been studied extensively.³⁻⁷ The coexistence line ends in a critical point around $T_c \approx (15-17) \times 10^3 \text{ K}$, a pressure of about $p_c \approx (50-70) \text{ GPa}$, and a density of about $\rho_c \approx (0.1-0.5) \text{ g/cm}^3$; see Ref. 30 for an overview. Extrapolation of our results to higher temperatures matches these predictions.

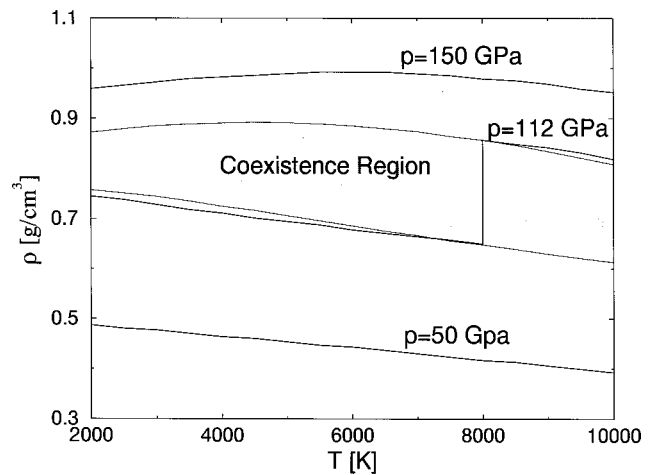


FIG. 3. Coexistence region and three isobars as function of the temperature.

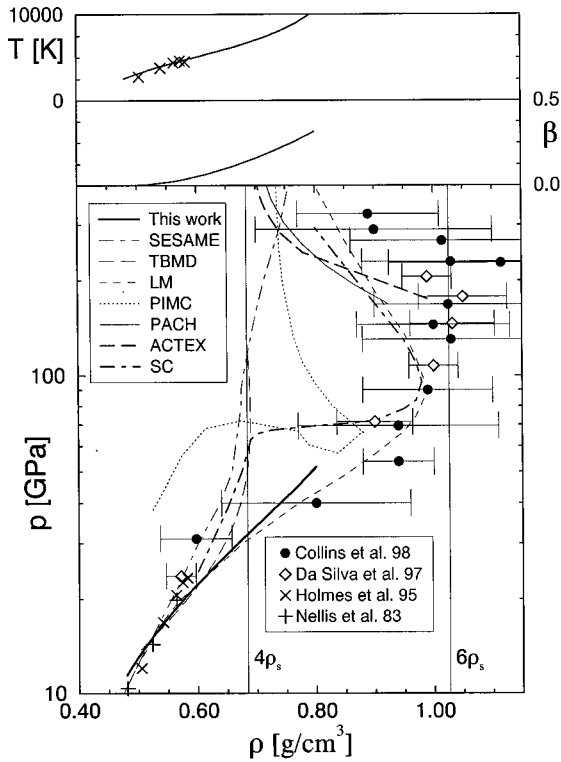


FIG. 4. Pressure p , degree of dissociation β , and temperature T along a single-shock Hugoniot curve of D_2 vs density: \diamond and \bullet denote data from laser-driven shock-wave experiments (Refs. 32 and 33), while \times and $+$ are taken from gas gun experiments (Refs. 24 and 25). The present results (thick solid line) are compared with Hugoniot curves derived from a semiempirical linear-mixing model (LM) (Ref. 9), the SESAME tables (Ref. 34), tight-binding molecular dynamics (TBMD) (Ref. 12), and path-integral Monte Carlo simulations (PIMC) (Ref. 35), from Padé approximations in a chemical picture (PACH) (Ref. 17), the activity expansion method (ACTEX) (Ref. 36), and the hydrogen equation of state (SC) given in Ref. 4.

To compare the results of the present EOS directly with available experimental data, we have calculated the pressure p , the degree of dissociation β , and the temperature T along a Hugoniot curve of D_2 using an initial pressure and density as typical for single shock experiments;^{25,32,33} see Fig. 4. Temperatures up to 10 000 K correspond to a maximum density of about 0.8 g/cm^3 . In this range our model is in good agreement with the experimental data³² and the linear-mixing (LM) model of Ross.⁹ Strong deviations from the behavior predicted by the SESAME tables³⁴ occur due to dissociation. The tight-binding molecular dynamics (TBMD) simulations¹² do not reproduce the strong compression between 30 GPa and about 100 GPa as observed experimentally. Applying the hydrogen EOS given by Saumon and Chabrier⁴ (SC) for the calculation of the Hugoniot curve, an almost abrupt compression at about 70 GPa occurs which is not verified by the experimental data. The path-integral Monte Carlo (PIMC) simulations³⁵ become increasingly reliable as the temperature increases, but fail to reproduce the neutral fluid behavior at low temperatures. At high tempera-

tures, our model recovers the Hugoniot curve for a highly ionized plasma, calculated by means of the Padé approximations in a chemical picture (PACH) for the EOS of the charged component used also here. In this area the PACH model shows a good agreement with the activity expansion (ACTEX) method of Rogers.³⁶ The results of the LM, ACTEX, SC, and PACH models are in reasonable agreement with the experimentally observed turnaround of the Hugoniot curve for high temperatures.

IV. CONCLUSIONS

In this paper, we have proposed an EOS for dense hydrogen plasma for $T \leq 10^4$ K which gives a realistic behavior for low (neutral molecular fluid) and high temperatures (fully ionized plasma). A thermodynamic instability occurs in the intermediate region that is connected with a first-order phase transition. The *plasma phase transition* describes a transition from a partially dissociated fluid to a partially ionized plasma. We have derived the corresponding coexistence line and the coexistence region for $T = (2-10) \times 10^3$ K. The coexistence line might end in a critical point as other theories have predicted.³⁻⁶ For a detailed study of the region near the critical point, the present EOS has to be extended to higher temperatures. Furthermore, the charged-neutral interaction has to be considered in addition.

Compared with previous approaches,³⁻⁷ the correlations in the dense, neutral component are now considered in a systematic way, going beyond rather approximative methods such as the hard-sphere reference system or perturbation theory. The applicability of the dissociation model for not too high temperatures and densities has been demonstrated by comparing the respective proton-proton distribution functions with results from computer simulations.³¹

As discussed above, the present EOS yields a first-order phase transition with a corresponding separation between two phases of different mass density and degree of ionization. This so-far hypothetical phase transition might be closely related to the experimentally observed electronic transition to metalliclike conductivities in fluid hydrogen.¹ The present EOS yields a transition pressure of about 120–110 GPa in that region. Numerical simulations^{14,16} also support the occurrence of a first-order phase transition in hydrogen. Such a behavior would be very similar to that of expanded fluid alkali metals where an electronic metal-insulator transition occurs near the critical point of the ordinary liquid-vapor phase transition; see Ref. 37. A final decision about the nature of the observed transition from a semiconducting fluid to a highly conducting phase at temperatures $T = (2-10) \times 10^3$ K requires still more precise experiments as well as more refined theories.

In order to check the accuracy of the present EOS, we have calculated the respective Hugoniot curves and compared with available data from recent shock-compression experiments^{32,33} as well as other theories.^{4,9,12,35,36} We have shown that our model—in the region of densities studied here ($\rho < 0.8 \text{ g/cm}^3$)—provides a good representation of the experimental data points and can well be compared with the results of the linear-mixing model of Ross.⁹

- ¹S.T. Weir, A.C. Mitchell, and W.J. Nellis, Phys. Rev. Lett. **76**, 1860 (1996).
- ²V. Ya. Ternovoi, A. S. Filimonov, V. E. Fortov, S. V. Kvitov, D. N. Nikolaev, and A. A. Pyalling, Physica B **265**, 6 (1999).
- ³W. Ebeling and W. Richert, Phys. Status Solidi B **128**, 467 (1985); Phys. Lett. **108A**, 80 (1985); Contrib. Plasma Phys. **25**, 431 (1985).
- ⁴D. Saumon and G. Chabrier, Phys. Rev. Lett. **62**, 2397 (1989); Phys. Rev. A **44**, 5122 (1991); **46**, 2084 (1992); D. Saumon, G. Chabrier, and H.M. Van Horn, Astrophys. J., Suppl. Ser. **99**, 713 (1995).
- ⁵M. Schlanges, M. Bonitz, and A. Tschtschjan, Contrib. Plasma Phys. **35**, 109 (1995).
- ⁶H. Reinholz, R. Redmer, and S. Nagel, Phys. Rev. E **52**, 5368 (1995).
- ⁷H. Kitamura and S. Ichimaru, J. Phys. Soc. Jpn. **67**, 950 (1998).
- ⁸W.J. Nellis, S.T. Weir, and A.C. Mitchell, Phys. Rev. B **59**, 3434 (1999).
- ⁹M. Ross, Phys. Rev. B **54**, R9589 (1996); **58**, 669 (1998); Contrib. Plasma Phys. **39**, 17 (1999).
- ¹⁰V.S. Filinov and G.E. Norman, Phys. Lett. **55A**, 219 (1975).
- ¹¹D. Hohl, V. Natoli, D.M. Ceperley, and R.M. Martin, Phys. Rev. Lett. **71**, 541 (1993); J. Kohanoff, and J.-P. Hansen, *ibid.* **74**, 626 (1995); Phys. Rev. E **54**, 768 (1996).
- ¹²L. Collins, I. Kwon, J. Kress, N. Troullier, and D. Lynch, Phys. Rev. E **52**, 6202 (1995); I. Kwon, L. Collins, J. Kress, and N. Troullier, *ibid.* **54**, 2844 (1996); T.J. Lenosky, J.D. Kress, L.A. Collins, and I. Kwon, Phys. Rev. B **55**, R11 907 (1997).
- ¹³D. Klakow, C. Toepffer, and P.-G. Reinhard, Phys. Lett. A **192**, 55 (1994); J. Chem. Phys. **101**, 10 766 (1994).
- ¹⁴M. Knaup, D. Klakow, P.-G. Reinhard, and C. Toepffer, in *Strongly Coupled Coulomb Systems*, edited by G.J. Kalman, J.M. Rommel, and K. Blagoev (Plenum, New York, 1998), p. 341.
- ¹⁵C. Pierleoni, D.M. Ceperley, B. Bernu, and W.R. Magro, Phys. Rev. Lett. **73**, 2145 (1994).
- ¹⁶W.R. Magro, D.M. Ceperley, C. Pierleoni, and B. Bernu, Phys. Rev. Lett. **76**, 1240 (1996).
- ¹⁷W. Ebeling, Contrib. Plasma Phys. **30**, 553 (1990); T. Kahlbaum and A. Förster, Laser Part. Beams **8**, 753 (1990).
- ¹⁸W. Ebeling, A. Förster, V.E. Fortov, V.K. Gryaznov, and A.Ya. Polishchuk, *Thermophysical Properties of Hot Dense Plasmas* (B.G. Teubner Verlagsgesellschaft, Stuttgart and Leipzig, 1991).
- ¹⁹A. Förster, T. Kahlbaum, and W. Ebeling, Laser Part. Beams **10**, 253 (1992).
- ²⁰A. Bunker, S. Nagel, R. Redmer, and G. Röpke, Phys. Rev. B **56**, 3094 (1997).
- ²¹A. Bunker, S. Nagel, R. Redmer, and G. Röpke, Contrib. Plasma Phys. **37**, 115 (1997); **37**, 469(E) (1997).
- ²²A. Förster and W. Ebeling, in *Physics of Nonideal Plasmas*, edited by W. Ebeling, A. Förster, and R. Radtke (B.G. Teubner Verlagsgesellschaft, Stuttgart and Leipzig, 1992), p. 100; T. Kahlbaum and A. Förster, Fluid Phase Equilibria **76**, 71 (1992).
- ²³M. Ross, F.H. Ree, and D.A. Young, J. Chem. Phys. **79**, 1487 (1983).
- ²⁴W.J. Nellis, A.C. Mitchell, M. van Thiel, G.J. Devine, R.J. Trainor, and N. Brown, J. Chem. Phys. **79**, 1480 (1983).
- ²⁵N.C. Holmes, M. Ross, and W.J. Nellis, Phys. Rev. B **52**, 15 835 (1995).
- ²⁶W. Ebeling, W.D. Kraeft, and D. Kremp, *Theory of Bound States and Ionization Equilibrium in Plasmas and Solids* (Akademie-Verlag, Berlin, 1976).
- ²⁷W. Stolzmann and T. Blöcker, Phys. Lett. A **221**, 99 (1996); Astron. Astrophys. **314**, 1024 (1996).
- ²⁸R. Redmer, G. Röpke, D. Beule, and W. Ebeling, Contrib. Plasma Phys. **39**, 25 (1999).
- ²⁹H.-K. Mao and R.J. Hemley, Rev. Mod. Phys. **66**, 671 (1994).
- ³⁰R. Redmer, Phys. Rep. **282**, 35 (1997).
- ³¹S. Nagel, R. Redmer, G. Röpke, M. Knaup, and C. Toepffer, Phys. Rev. E **57**, 5572 (1998).
- ³²L.B. Da Silva, P. Celliers, G.W. Collins, K.S. Budil, N.C. Holmes, T.W. Barbee, Jr., B.A. Hammel, J.D. Kilkenny, R.J. Wallace, M. Ross, R. Cauble, A. Ng, and G. Chiu, Phys. Rev. Lett. **78**, 483 (1997).
- ³³G.W. Collins, L.B. Da Silva, P. Celliers, D.M. Gold, M.E. Foord, R.J. Wallace, A. Ng, S.V. Weber, K.S. Budil, and R. Cauble, Science **281**, 1178 (1998).
- ³⁴G.I. Kerley (unpublished).
- ³⁵B. Militzer, W. Magro, and D. Ceperley, in *Strongly Coupled Coulomb Systems*, edited by G.J. Kalman, J.M. Rommel, and K. Blagoev (Plenum, New York, 1998), p. 357; B. Militzer (private communication).
- ³⁶F.J. Rogers, Astrophys. J. **310**, 723 (1986); F.J. Rogers, F.J. Swenson, and C.A. Iglesias, *ibid.* **456**, 902 (1996).
- ³⁷F. Hensel, J. Phys.: Condens. Matter **2**, SA33 (1990); F. Hensel and P.P. Edwards, Chem.-Eur. J. **2**, 1201 (1996).